Journal of Physics B: Atomic, Molecular and Optical Physics

PAPER

Study of inelastic processes in Li^+–Ar, K^+–Ar, and Na^+–He collisions in the energy range 0.5–10 keV

To cite this article: Ramaz A Lomsadze *et al* 2017 *J. Phys. B: At. Mol. Opt. Phys.* **50** 215002

IOP Publishing Journal of Physics B: Atomic, Molecular and Optical Physics
J. Phys. B: At. Mol. Opt. Phys. **50** (2017) 215002 (13pp) https://doi.org/10.1088/1361-6455/aa8dd3

Study of inelastic processes in Li^+–Ar, K^+–Ar, and Na^+–He collisions in the energy range 0.5–10 keV

Ramaz A Lomsadze[1], Malkhaz R Gochitashvili[1], Roman Ya Kezerashvili[2,3] and Michael Schulz[4]

[1] Tbilisi State University, Tbilisi, 0179, Georgia
[2] Physics Department, New York City College of Technology, The City University of New York, Brooklyn, NY 11201, United States of America
[3] The Graduate School and University Center, The City University of New York, New York, NY 10016, United States of America
[4] Missouri University of Science and Technology, Rolla, MO 65409, United States of America

E-mail: rkezerashvili@citytech.cuny.edu

Received 16 March 2017, revised 15 September 2017
Accepted for publication 20 September 2017
Published 23 October 2017

Abstract

Absolute cross sections are measured for charge-exchange, ionization, and excitation processes within the same experimental setup for the Li^+–Ar, K^+–Ar, and Na^+–He collisions in the ion energy range of 0.5–10 keV. The results of the measurements and schematic correlation diagrams are used to analyze and determine the mechanisms for these processes. The experimental results show that the charge-exchange processes occur with high probabilities and electrons are predominantly captured in ground states. The contributions of various partial inelastic channels to the total ionization cross section are estimated, and a primary mechanism for the process is identified. In addition, the energy-loss spectrum is applied in order to estimate the relative contribution of different inelastic channels, and to determine the mechanisms for the ionization and for some excitation processes of Ar resonance lines for the K^+–Ar collision system. The excitation cross sections for the helium and for the sodium doublet lines for the Na^+–He collision system both reveal some unexpected features. A mechanism to explain this observation is suggested.

Keywords: ion-atom collusion, absolute cross sections, charge-exchange processes, ionization processes, excitation processes

(Some figures may appear in colour only in the online journal)

1. Introduction

The investigation of the charge-exchange, ionization and excitation processes in collisions of alkali-metal ions with atoms of rare gases is of great importance, not only in basic atomic collision physics, e.g. for understanding the collision dynamics and mechanisms of reactions, but also in other fields as plasma physics, surface science and astrophysics. Research on alkali-metal ion collisions with rare gas atoms has been carried out with different experimental approaches and several methods [1–21]. However, the available data for the absolute cross sections of the abovementioned processes are not always consistent with each other, and in some cases are unreliable. A brief survey of processes occurring in alkali-metal ion impact with atoms of rare gases shows that today most of the experimental results are either provided in arbitrary units, or pertain to a restricted energy interval. These circumstances call for detailed investigation of the primary mechanisms for various inelastic processes in the alkali ion–rare gas atom collisions. So far, we have studied inelastic processes in the K^+–He, Na^+–Ne, Na^+–Ar, Ne^+–Na, and Ar^+–Na collisions [16, 19, 21].

The present work is focused on a detailed study of charge-exchange, ionization and excitation processes induced

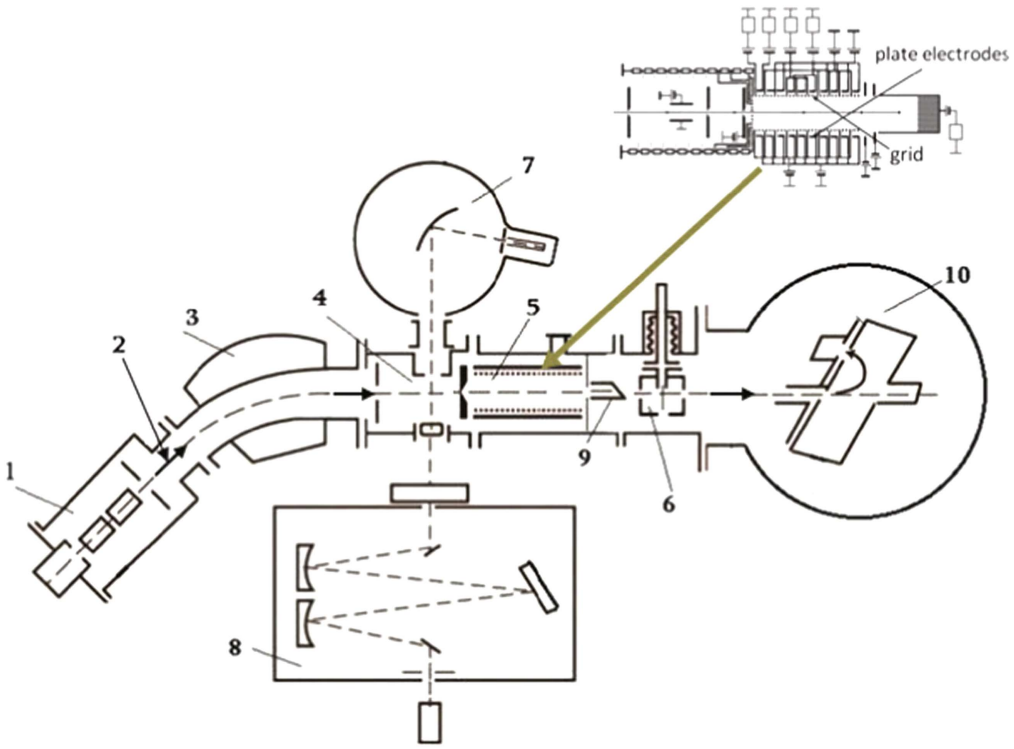

Figure 1. Schematic diagram of the experimental set up: 1—ion source, 2—ion beam, 3—magnet mass-analyzer, 4—first collision chamber, 5—second collision chamber, 6—third collision chamber, 7—vacuum ultraviolet spectrometer, 8—visible spectrometer, 9—Faraday cup, 10—electrostatic analyzer. The insert at the upper right corner shows the device used for a refined version of the capacitor method.

by collisions of closed-shell alkali-metal ions of Li^+, K^+, and Na^+ with the Ar and He atoms in the energy range of 0.5–10 keV. These processes are all studied under the same experimental conditions. The products of the charge-exchange reaction can be in the ground states or in different excited states. The ionization processes for the target atoms may include different channels for the excitation of the ions of target atoms or/and incident ions, as well as the excitation of autoionization states of the target atom that leads to its ionization. The excitation processes may also include different channels for excitation of the K^+ and/or Ar atom, and the Na^+ ion or/and He atom, respectively. To find contributions of various channels, we perform measurements of absolute differential and total cross sections and energy-losses for charge-exchange, ionization and excitation processes in Li^+−Ar, K^+−Ar, and Na^+−He collisions. The experimental data and the schematic correlation diagrams are used to analyze and estimate the contributions of various channels to the charge-exchange, ionization and excitation processes. The final objective of this work is the determination of dominant mechanisms for these processes in the energy range of 0.5–10 keV.

This paper is organized in the following way. In section 2, the experimental techniques and measurement procedures, are described, and three different experimental methods of measurements are presented. The description of our results and a comparison to results of previous studies for the charge-exchange, ionization and excitation in the Li^+−Ar, K^+−Ar, and Na^+−He collisions are given in section 3. The discussion of the experimental results and the identification of the mechanisms for various reaction channels are presented in section 4. Finally, in section 5, we summarize our investigations and present the conclusions.

2. Experimental techniques and measurement procedures

The main schematic set-up used in current experiments is shown in figure 1. The methods used for measurements of excitation, charge-exchange and ionization processes are the following: (i) optical spectroscopy; (ii) refined version of the capacitor; (iii) collision spectroscopy. An important feature of our experimental approach is that the quality of the beam, as well as the experimental conditions for all processes under investigation, always remain identical. The basic approach for measurements of inelastic processes in alkali-metal ions with rare gas atoms collision systems was described previously in [19]. Therefore, only the details of the apparatus with a description of methods, and measurement procedures, will be given here.

A beam of the Li^+, K^+, or Na^+ ions emitted from a surface-ionization ion source is accelerated, formed, and focused by an ion-optics system, which includes quadruple lenses and collimation slits. After the beam passes through a magnetic mass spectrometer, it enters the collision chambers containing Ar or He target gases. When the beam of ions passes through the first collision chamber, excitation processes are measured, while in the second collision chamber the charge-exchange and ionization processes are measured.

After being collimated through a slit, the ion beam enters into the third collision chamber and then passes into a 'box' type electrostatic analyzer.

2.1. The measurements of excitation cross sections are performed when the ion beam passes through the first collision chamber. The radiation emitted by the excited atoms is viewed perpendicularly to the beam by spectrometers. The spectral analysis of the radiation is performed by optical and vacuum ultraviolet spectrometers. The linear polarization of the emission in the visible spectrum is analyzed by both a Polaroid and a mica quarter-wave phase plate. The polarization of the radiation in the vacuum ultraviolet region is not taken into account. The radiation is recorded by the secondary electron multiplier, used under integrating or pulse-counting conditions. The main issue in finding the excitation cross section is to determine the relative and absolute spectral sensitivity of the light-recording system. We determine the absolute excitation cross sections by measuring the signal due to emission of molecular bands and atomic lines excited by electrons in collisions with H_2, N_2, O_2 and Ar [23]. To this end, an electron gun was placed directly in front of the entrance slit of the collision chamber. The relative spectral sensitivity and the value of the absolute cross sections were obtained by comparing the cross sections for the same lines and molecular bands reported in [24, 25]. For example, in the visible spectrum this was done by measuring the photomultiplier output signal caused by the first negative ($B^2\Sigma u^+ - X^2\Sigma g^+$ transition) and Meinel ($A^2\Pi u^+ - X^2\Sigma g^+$ transition) band system in the ionized nitrogen molecule N_2^+ [26]. These bands cover the wavelength interval between 423.6 and 785.4 nm. The output signal is normalized to the (0.1) band ($\lambda = 427.8$ nm), which has the highest intensity in this range. The absolute uncertainties in the excitation cross section for the $K^+ - Ar$ and $Na^+ - He$ collision systems are estimated to be 15%, and the uncertainty of relative measurements is about 5%.

2.2. The charge-exchange and ionization cross section were measured when the beam passed the second collision chamber, by a refined version of the capacitor method (the insert in figure 1) [13]. This method represents a direct measurement of positively charged ions and free electrons as the primary beam passes through the target gas. Obviously, the measured quantities are related to the capture and ionization cross sections [19]. The uncertainties in the measurements of the charge-exchange cross sections for the $Li^+ - Ar$, $K^+ - Ar$, and $Na^+ - He$ collision systems are estimated to be 7%, 15%, and 10%, respectively, while the uncertainties in the measurements of the ionization cross sections are estimated to be 12%, 10%, and 15%, respectively. These uncertainties are caused primarily by the uncertainties in the measurements of the absolute cross sections for production of positively charged ions and free electrons as the primary beam passes through the target, and by the uncertainty in the measurement of the target gas pressure in the collision chamber.

2.3. The measurements of energy-loss spectra and differential cross sections are performed when the beam passes the third collision chamber, by the collision spectroscopy method [22], using the electrostatic analyzer. The energy resolution of this analyzer is $\Delta E/E = 1/500$. The voltage applied to the analyzer is scanned automatically which allows investigation of the energy-loss spectra in the energy range of 0–100 eV. The differential cross section is measured by the electrostatic analyzer that rotates around the center of collision in the angular range of 0°–20°. The laboratory angle is determined with respect to the primary ion beam axis with an accuracy of 0.2°. Such a tool provides us with the second way to determine the total cross sections and to compare them with the results obtained by the refined version of the capacitor method [13]. In addition, the measured energy-loss spectra provide detailed information related to the intensity of inelastic processes in the charge-exchange, ionization and excitation reactions.

3. Results of experimental measurements

To have a clear understanding of the realized processes, it is reasonable to treat the results of measurements by taking into consideration the internal structure of colliding systems and kinematic effects as well. Therefore, we arrange our experimental results in two possible ways: (i) for each collision system, namely for $Li^+ - Ar$, $K^+ - Ar$, and $Na^+ - He$, we present all measured inelastic processes; (ii) for each inelastic process, namely for the charge-exchange, the ionization, and excitation reactions, we present the results of measurements for all the collision systems.

The results of our measurements for the absolute charge-exchange, ionization, and excitation cross sections for $Li^+ - Ar$, $K^+ - Ar$, and $Na^+ - He$ collisions are presented in figure 2. The charge-exchange cross sections have almost a flat energy dependence, while the ionization cross sections increase monotonically with energy, and the excitation function in the $Na^+ - He$ shows an oscillatory behavior.

Comparison of the results presented in figure 2(a) for the $K^+ - Ar$ collision system shows that the charge-exchange process in ground $4s$ state is dominant. The difference in magnitude between the charge-exchange in the ground state and ionization cross sections at $E = 0.5$ keV attains a factor of three. With the increase of the ion energy, the ionization cross section increases monotonically, and at energy of 6 keV it coincides with the charge-exchange cross section. The cross section for excitation to the Ar($4s$) and K($4p$) states is about 30 times less in comparison to the charge-exchange and ionization cross sections in the entire energy interval.

Comparison of the results for the charge-exchange and ionization processes for the $Li^+ - Ar$ collision system in figure 2(b) (the excitation cross section was not measured for this collision system) shows that the difference in the cross sections at $E = 3$ keV reaches one order of the magnitude. As the ionization cross section increases monotonically with the energy of the Li^+ ion, the difference reduces, and at the energy of 7 keV it is only a factor of three.

Comparison of the results presented in figure 2(c) for the $Na^+ - He$ shows that the charge-exchange process is also dominant. The ratio of the charge-exchange and ionization

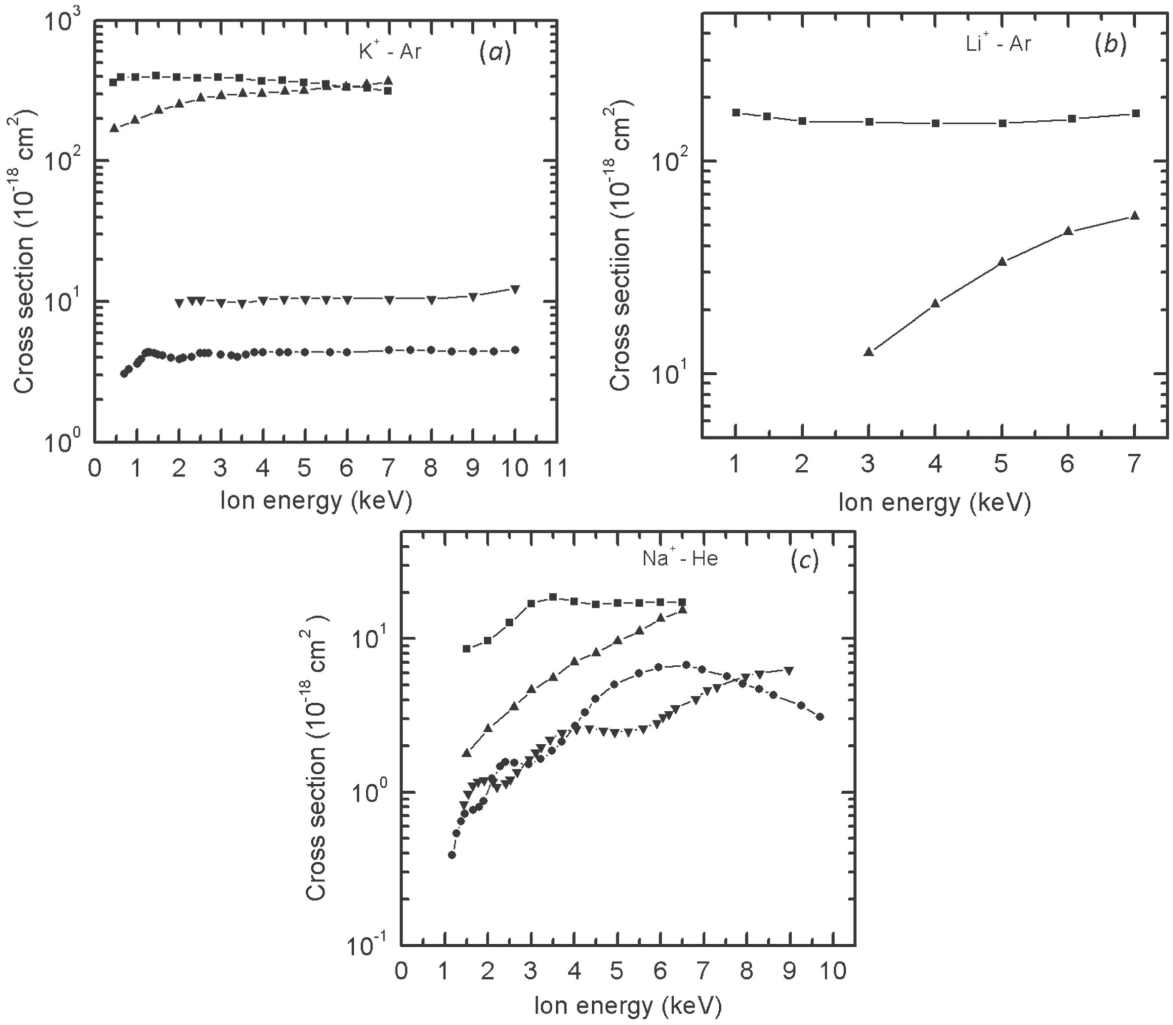

Figure 2. Dependences of the absolute charge-exchange, the absolute ionization, and the excitation cross sections on energy of an incident ion. (a)—K^+-Ar collisions, data: ■—electron capture to the ground potassium K(4*s*) state; ▲—ionization of the Ar atom; ▼—excitation function of the resonance argon atomic line $\lambda = 106.7$ nm, $3p^5 4s - 3p^6$ transition; •—electron capture to the excited resonance K(4*p*) state, $\lambda = 766.5$—769.8 nm, transition $4p - 4s$. (b)—Li^+-Ar collisions, data: ■—electron capture to the ground lithium Li(2*s*) state; ▲—ionization of the Ar atom. (c)—Na^+-He collisions, data: ■—electron capture to the ground sodium Na (3*s*) state; ▲—ionization of the He atom; ▼—excitation of the He(2*p*) state, $\lambda = 58.4$ nm corresponding to the $2p - 1s$ transition; •—electron capture to the excited state of Na(3*p*) of the resonance sodium doublet lines $\lambda = 589.0$ nm and $\lambda = 589.6$ nm for the transition $3p - 3s$.

cross sections at energy $E = 1.5$ keV attains the factor of five. With the increase of energy the ionization cross sections increases monotonically and the difference in magnitude between the cross sections decreases. At $E = 6.5$ keV, the cross sections practically coincide with each other. As for the excitation cross sections for the sodium and helium atomic lines, they are smaller than the cross sections for the ionization and the charge exchange processes.

To proceed with the analysis of mechanisms of processes, it is reasonable to rearrange the experimental data in figure 2, and present the total cross sections for the charge-exchange, ionization, and excitation processes separately for each collision system. This presentation also allows us to understand the dependence of the cross sections on the mass ratio of colliding particles. The energy dependences of the absolute cross sections for the charge-exchange, ionization and excitation processes are presented in figures 3–5. Figure 6 represents a typical example of the energy-loss spectrum for the K^+-Ar collision system. Analysis of figures 3–5 shows marked differences for the energy dependences of the cross sections for the various processes.

3.1. The cross sections for electron capture to the ground state of lithium Li (2*s*), potassium K(4*s*), and sodium Na (3*s*) for Li^+-Ar, K^+-Ar, and Na^+-He collision systems, respectively, are presented in figure 3. In the same figure the charge-exchange for the excited resonance K (4*p*) state for the K^+-Ar, and Na (3*p*) state for the Na^+-He are presented. Among inelastic processes, the charge-exchange has the largest cross section. The comparison of the charge-exchange cross sections for the K^+-Ar collision system with the results from [27] at $E = 350$ eV and [8] at $E = 2$ keV are in satisfactory agreement within the range of the experimental uncertainties. Our results for the Na^+-He charge-exchange processes can be compared with the cross section obtained in differential scattering experiments [20] at $E = 1.5$ keV. This comparison shows that here, the discrepancy amounts to a

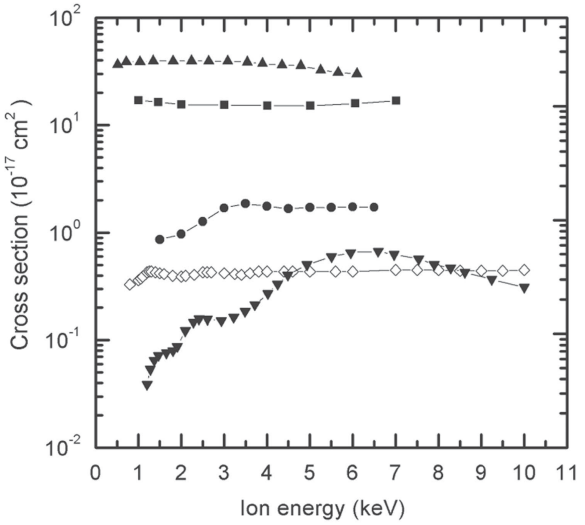

Figure 3. Dependences of the absolute charge-exchange cross sections on energy of Li^+, K^+ and Na^+ ions in Li^+-Ar , K^+-Ar, and Na^+-He collisions. Data: ▲—electron capture to the ground potassium K($4s$) state for the K^+- Ar system; ◊—electron capture to the excited resonance K($4p$) state ($\lambda = 766.5 - 769.8$ nm, transition $4p - 4s$) for the K^+-Ar collision; ■—electron capture to the ground lithium Li ($2s$) state for the Li^+-Ar system; •— electron capture to the ground sodium Na ($3s$) state for the Na^+-He system; ▼—electron capture to the excited resonance sodium Na ($3p$) state ($\lambda = 589.0 - 589.6$ nm, transition $3p - 3s$) for the Na^+-He system.

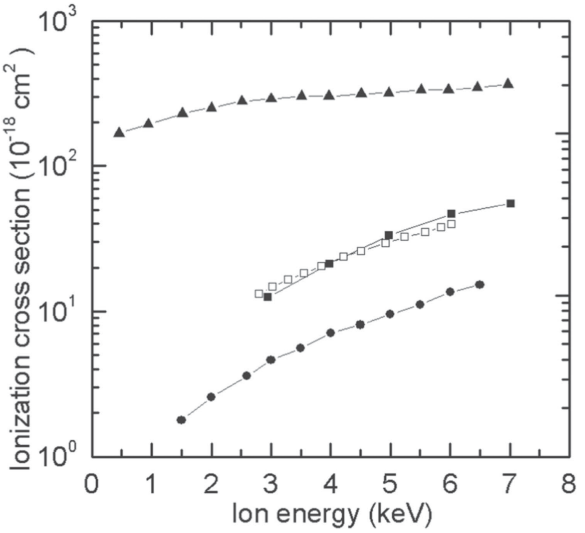

Figure 4. Dependences of the absolute ionization cross sections on energy of Li^+, K^+, and Na^+ ions in the Li^+-Ar, K^+- Ar, and Na^+-He collisions. Data: ▲—K^+-Ar; ■ —Li^+-Ar; •— Na^+-He; □—present calculations.

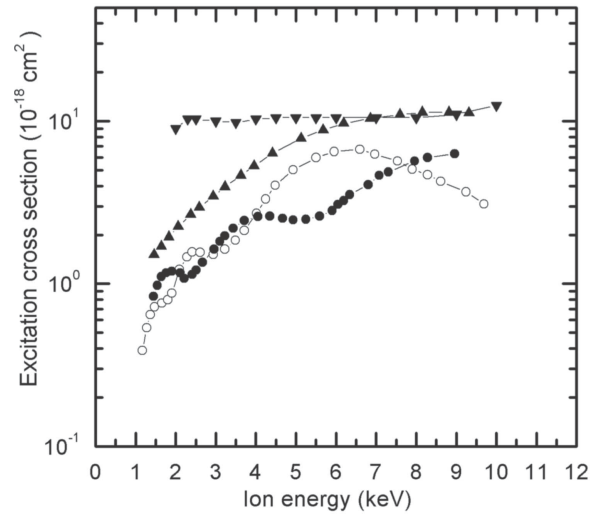

Figure 5. Excitation cross sections for the resonance argon atomic line for the K^+- Ar collision system, and for the resonance lines of sodium doublet and helium atom in the Na^+-He collision. Data: ▼—excitation cross section for the resonance argon atomic line $\lambda = 106.7$ nm, corresponding to the transition $3p^5 4s - 3p^6$ in the K^+- Ar collision system; •—excitation cross section for the resonance helium atomic line $\lambda = 58.4$ nm corresponding to the $2p - 1s$ transition in the Na^+-He collision system; ∘—excitation cross section of the resonance sodium doublet lines $\lambda = 589.0$ nm and 589.6 nm for the transition $3p - 3s$ in the Na^+- He system; ▲—the sum of the excitation cross sections of the resonance helium atomic line (•) and resonance sodium doublet lines (∘) for the Na^+-He collision.

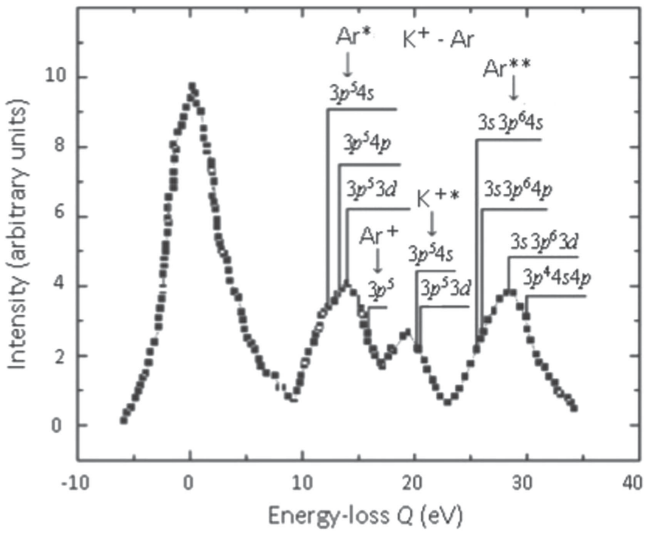

Figure 6. Typical energy-loss spectrum in laboratory reference system for K^+-Ar collisions measured at $E = 2$ keV collision energy and $\theta = 3.5^0$ scattering angle.

factor of three. At $E \leqslant 1.5$ keV, our excitation cross section for the K($4p$) state in the K^+-Ar collision is in good agreement with the earlier data [9]. Interestingly enough, the charge exchange cross section for the Na^+-He collisions with the electron capture to the excited resonance sodium Na($3p$) state features an oscillatory behavior that is observed for the first time. Such oscillatory behavior is a result of phase-interference effects [2, 28, 29] in Na^+-He inelastic collision, and is discussed below, in section 4.

The results for the charge-exchange processes in figure 3 show that for a quasisymmetric system (approximately equal colliding masses, like the K^+-Ar pair) the cross section in the entire energy range is greater than one for a largely asymmetric system (largely unequal colliding masses, like the Li^+-Ar and Na^+-He pairs). The cross section ratio for

electron capture to the 4*s*, 2*s*, and 3*s* ground states for the K^+-Ar, Li^+-Ar and Na^+-He collision systems attains roughly the value of 4:2:1. Moreover, when the mass of the incident particle for the largely asymmetric system is bigger than the mass of target particle, the charge-exchange cross section is smaller. This result can be explained in the framework of the quasi-molecular approach. Cross sections of inelastic processes depend on the internuclear distances at which potential curves approach or cross each other. To the larger distance corresponds the larger cross section. When inelastic process is induced by collisions of closed-shell alkali-metal ions with rare gas atoms, the electron transition takes place effectively at the distance $R = r_i + r_a$, where r_i and r_a are the radii of the ion and atom, respectively. Based on the data reported in [14, 17, 20], effective interaction distances for the K^+-Ar, Li^+-Ar, and Na^+-He collision systems are 1.19×10^{-10} m, 0.83×10^{-10} m and 0.63×10^{-10} m, respectively. Hence, the maximum cross section is expected for the K^+-Ar collision system, and the minimum for the Na^+-He collision system.

3.2. The ionization cross section for the Li^+-Ar, K^+-Ar, and the Na^+-He collision systems are shown in figure 4. The comparison of the ionization cross section for K^+-Ar collisions that we obtained is in good agreement with measurements [6] at $E = 2$ keV. The experimental results for the ionization cross section for the Li^+- Ar collision system are in an excellent agreement with our calculations based on [30]. It is important to mention that at high energy the ionization cross section for the Li^+-Ar collision system is suppressed by the direct one electron excitation of the Ar atom in the 4*s*, 4*p* and 3*d* states. This follows from experimental measurements reported in [14], and can be confirmed by the correlation diagram in figure 7.

The results for the ionization processes presented in figure 4 show that the cross section in the entire energy range in the case of the quasisymmetric collision system (K^+-Ar) is greater than cross sections for the largely asymmetric collision system (Li^+-Ar and Na^+-He). The ionization cross sections ratio for the K^+-Ar, Li^+-Ar and Na^+-He systems attains roughly the value of 100:10:2.

3.3. The results of excitation cross sections for the K^+- Ar and Na^+-He collisions are presented in figure 5.

For the Na^+-He collision, we performed measurements for two channels: one channel is the capture of the electron in the excited resonant state 3*p* of the sodium atom in the charge exchange process and the other inelastic channel is the resonant excitation of the target atom He in the 2*p* state. The observation of the oscillatory structure of the cross sections for the resonance helium atomic line ($\lambda = 58.4$ nm corresponding to the $2p - 1s$ transition) and the resonance sodium doublet lines ($\lambda = 589.0$ nm and 589.6 nm for the transition $3p - 3s$) in the Na^+-He system is of particular interest. This oscillatory behavior of the cross sections is a result of phase-interference effects [2, 28, 29] in Na^+-He inelastic collision, and it will be addressed in section 4. Comparison of the excitation cross section for the helium atom with the results reported in [3] shows that the energy dependence with a pronounced oscillatory behavior on the excitation cross section of the helium atom is the same, and the oscillations are in phase. However, there are considerable discrepancies in magnitude of the excitation cross sections. The results for the cross section in our measurements are more than one order higher. It is difficult to compare our results for the excitation of the Ar resonance 4*s*, line $\lambda = 106.7$ nm with the results from [2] obtained in the range of 1–3 keV because the authors considered the excitation of the Ar resonance 4*s* as the sum of lines $\lambda = 104.8$ nm and $\lambda = 106.7$ nm. Our results of the helium atomic resonance line are three times those from [20] at $E = 1.5$ keV.

In figure 5, we also present the sum of the cross sections for the resonance helium line, transition to the $2p - 1s$ and the resonance sodium doublet lines, transition to the $3p - 3s$, in the Na^+-He system. The comparison of the results in figure 5 show that the ratio of the cross section for the resonance argon atomic line (K^+-Ar) and the sum of the excitation cross sections of the resonance helium atomic line and the resonance sodium doublet lines at $E = 1.5$ keV reaches a factor of 5. The cross section in the case of the quasisymmetric collision system (K^+-Ar) is greater than that of the largely asymmetric collision system (Na^+-He). By increasing the collision energy the sum of the excitation cross sections increases monotonically. In the energy range of 6–10 keV, the difference between them vanishes, and the ratio of the cross sections equals 1 up to 10 keV.

3.4. Generally we measure the energy-loss spectrum for the K^+-Ar collision at different fixed angles in the range of 1^0–7^0. Figure 6 shows a typical energy-loss spectrum with well-pronounced inelastic channels for the K^+-Ar collision system at $E = 2$ keV and $\theta = 3.5^0$. In the present study, this spectrum will be used to explore dominant mechanisms in the K^+-Ar collisions. The first peak of the spectrum with zero energy loss corresponds to the elastic scattering. The second one corresponds to the single electron excitation of the argon atom into $3p^5 4s$, $3p^5 4p$ and $3p^5 3d$ states, with the energy-loss *Q* within 11.6–14.0 eV, and a single ionization of the Ar atom in the state $3p^5$ for the energy loss of 15.7 eV. The third peak corresponds to the excitation of K^+ ion into the 4*s* and 3*d* states with the energy losses of 16–22 eV, while the fourth one corresponds to the excitation of autoionization states of the Ar atom with the excitation of one 3*s* electron or two 3*p* electrons, and to ionization with the excitation of the Ar, with the energy losses of 25–32 eV. Measurements of energy-loss spectrum for each scattering angle of the incident ions at the given energy allow us to estimate the relative contribution of different inelastic channels, determine the differential cross section, find the total cross section, and compare the total cross section with the total cross section measured by the refined capacitor method [13]. In our study, this approach is applied to determine the mechanism for the ionization processes, and for some excitation processes of Ar atoms in the K^+-Ar collision. The results are presented in section 4.

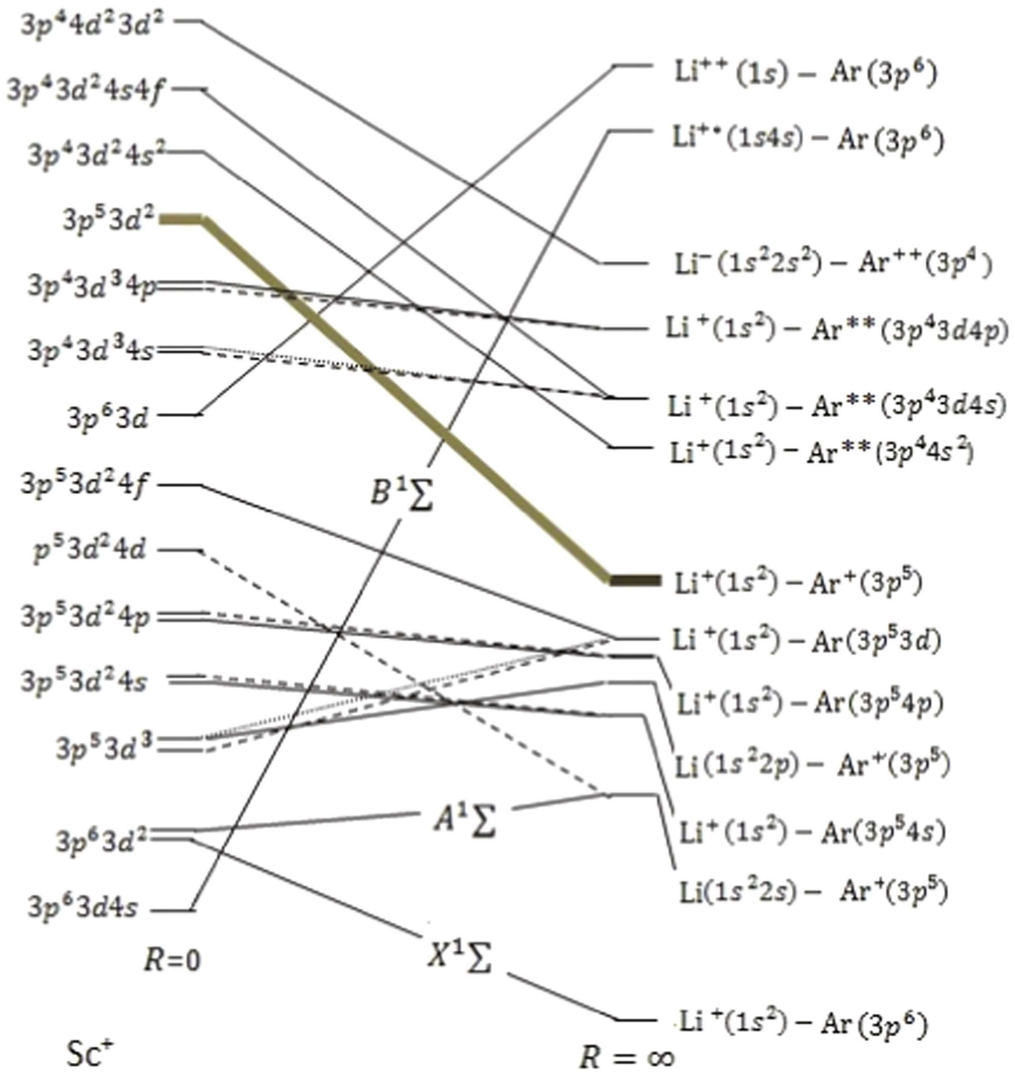

Figure 7. Schematic correlation diagram for some states of the Li^+-Ar collision system. Solid lines indicate Σ states, dashed lines indicate Π states.

4. Discussion of experimental results and mechanisms of processes

4.1. Charge exchange in $Li^+ - Ar$, $K^+ - Ar$, and $Na^+ - He$ collision systems

We use the experimental data for the individual inelastic channels, along with the corresponding schematic correlation diagrams, to establish the mechanism for the charge-exchange processes for the Li^+-Ar, K^+-Ar, and Na^+-He collision systems.

4.1.1. $Li^+ - Ar$ collisions. The results of the charge-exchange cross sections for the Li^+-Ar collision system are presented in figure 3. The dependence of the cross section on the energy of Li^+ ions is weak, and its average value is 1.4×10^{-16} cm^2.

The inelastic differential cross section measurements for the Li^+ ion collisions with rare gases have been reported in the keV energy range in [31]. The authors presented calculations for the potential curves of Σ symmetry, corresponding to the ground state of the system and the one- and two-electron excitation states of colliding particles. From the calculations [31] it follows that there are two coupling regions where non-adiabatic transitions may cause charge-exchange: one at internuclear distance $R \sim 1.5$ a.u., and the other at $R \leqslant 0.5$ a.u. Also the authors suggest that in both cases, the most probable mechanism of the charge-exchange process is the transition from the ground state of the system to the state corresponding to the electron capture into the ground state of lithium Li($1s^2 2s$). Our correlation diagram in figure 7 justifies that hypothesis. The transition between the terms $Li^+(1s^2) + Ar(3p^6)$ and $Li(2s) + Ar^+(3p^5)$ at the non-adiabatic region, corresponding to the internuclear distance $R \sim 1.5$ a.u., has been also observed in the measurements [31] for differential cross sections. However, the transition at $R \leqslant 0.5$ a.u. was not investigated in [31], since the process was studied only up to 25 keV deg., which means that the particles approach each other only up to $R \geqslant 0.75$ a.u. We integrate the differential cross section given in [31] at the energy of $E = 3$ keV to estimate the contribution of the transition at $R \leqslant 0.5$ a.u. to the total charge-exchange cross section, and compare it with our result. The comparison

shows that the results are consistent within the experimental uncertainties. Therefore, one can conclude that the contributions from transitions at $R \leqslant 0.5$ a.u. to the charge-exchange cross section is negligible, while the contribution from the transition at $R \sim 1.5$ a.u. to the charge-exchange cross section is dominant. A possible reason for the importance of this region, where the terms of $X^1\Sigma$ and $A^1\Sigma$ approach each other energetically, is the prevalence of the attraction between the Ar^+ ion and Li atom due to polarization, which overcomes the repulsion caused by the exchange interaction at those distances.

4.1.2. $K^+ - Ar$ collisions. To determine the mechanism for the K^+-Ar collisions, we compared the total charge-exchange cross section presented in figure 3 with that corresponding to the decay of excited resonance $K(4p)$ state of the potassium atom. Taking into account the selection rules and the ratio of oscillator strengths for the transitions, we find that the decay of any of the excitation levels of the potassium atom culminates, in about half of the cases, with a transition of the atom into a resonant state, which then decays. Thus, the doubled de-excitation cross section of the potassium atom gives an indication of the capture cross section in the excited state. The comparison of these two sets of our results shows that the contribution to the cross section from capture of an electron into the excited $4p$ state of potassium atom to the total charge-exchange cross section is small. Thus, the main contribution is related to the capture of the electron into the $4s$ ground state. However, the energy dependence of these cross sections is the same: The cross sections reach their maxima at $E \sim 1$ keV, and vary slowly in a wide energy range. The experimental results for the K^+-Ar collision that leads to the charge-exchange can be explained qualitatively in terms of the schematic correlation diagram for molecular orbitals that is given in [32] figure 5. The analysis of our results shows that the capture to the $4s$ ground and $4p$ excited states of the potassium atom are competing processes. This conclusion is supported by the fact that the terms corresponding to these states are populated from the same initial state term. Moreover, the parameters of the quasi-crossing region are such that the emission maxima occur at equal velocities. Substantial discrepancies between the magnitudes of the cross section are linked to the crossing point R of molecular terms, and can probably be explained by the fact that the processes occurred in different crossing points R of molecular terms. At first the $4s$ ground state at large internuclear distance R is populated, and after that the $4p$ excited state is populated at comparatively smaller distances R. Thus, one can conclude that charge-exchange into the $4s$ ground state and $4p$ excited state of the potassium atom involves the Landau–Zener type interaction, and occurs in the region of the quasi-crossing of the initial $K^+(3p^6)-$ Ar $(3p^6)$ and charge transferred $K(4s)$ + Ar $(3p^6)$ and/or $K(4p)$ + Ar $(3p^6)$ terms.

4.1.3. $Na^+ - He$ collisions. Two sets of experimental results are obtained in our study for charge exchange processes in Na^+-He collisions: one by the refined version of the capacitor method for measuring the total charge exchange cross sections of the processes

$$Na^+ + He \rightarrow Na(2p^6 3s) + He^+(1s), \quad (1)$$

$$\rightarrow Na(2p^6 3p) + He^+(1s), \quad (2)$$

$$\rightarrow Na(2p^6 3d) + He^+(1s), \quad (3)$$

when the sodium atom can be in various states, and the second one by optical measurements for the excitation into the states of $Na(2p^6 3p)$ and $Na(2p^6 3d)$. The comparison of these results shows that the fraction of the total cross section related to the sodium excited atom via channel (2) is roughly 10% of the total cross section. The contribution of channel (3) is negligible. Therefore, the charge-exchange processes in this study is mostly attributed to channel (1) with an electron capture to the ground state of the projectile. One can see from the correlation diagram in figure 8 that the charge-exchange processes to the $2p^6 3s$ ground state of sodium atom can occur due to the direct pseudo-crossing of the final state term $Na(2p^6 3s) + He^+(1s)$ with the initial state term $Na^+(2p^6) + He(1s^2)$. Since both the $Na^+(2p^6) + He(1s^2)$ and $Na(2p^6 3s) + He^+(1s)$ states have only Σ symmetry, it follows that the $\Sigma - \Sigma$ transition plays a dominant role in the charge-exchange process. In [20] an estimation was given for the contribution of various inelastic channels in the Na^+-He collisions to charge-exchange processes at energy $E = 1.5$ keV. The authors of [20] show that the direct one-electron target excitation in the reaction $Na^+ + He \rightarrow Na^+ + He^*(1s2s) + 20.6$ eV and charge exchange into the $3s$ ground state in the process $Na^+ + He \rightarrow Na\ (2p^6 3s) + He^+ + 19.44$ eV occur with high probabilities.

4.2. Ionization in $Li^+ - Ar$, $K^+ - Ar$, and $Na^+ - He$ collisions

4.2.1. $Li^+ - Ar$ collisions. To determine the mechanism of the ionization in Li^+-Ar collisions we use the electron energy spectra obtained in the present study, the differential cross section presented in [31] and a schematic correlation diagram shown in figure 7. We construct the correlation diagram according to the rules given in [32]. Our measurements show that the liberation of electrons with energies less than 10 eV is characteristic for the ionization in Li^+-Ar collisions. We estimate the contribution of several inelastic processes which result in the emission of slow electrons to the total ionization cross section. To estimate the fraction of the electrons coming from the autoionization states of Ar atoms to the ionization cross section, the differential cross section from [31] have been used. The integration of the corresponding differential cross section shows that the contribution of these processes to the total ionization cross section is about 17%. Small contributions from atomic autoionization into the total ionization processes follow also from the analyses of the correlation diagram in figure 7. None of the autoionization terms have an immediate crossing point with the ground state term and hence, as one would expect, their population occurs with small probabilities.

To the best of our knowledge there is no experimental data in the literature which could be used to estimate other

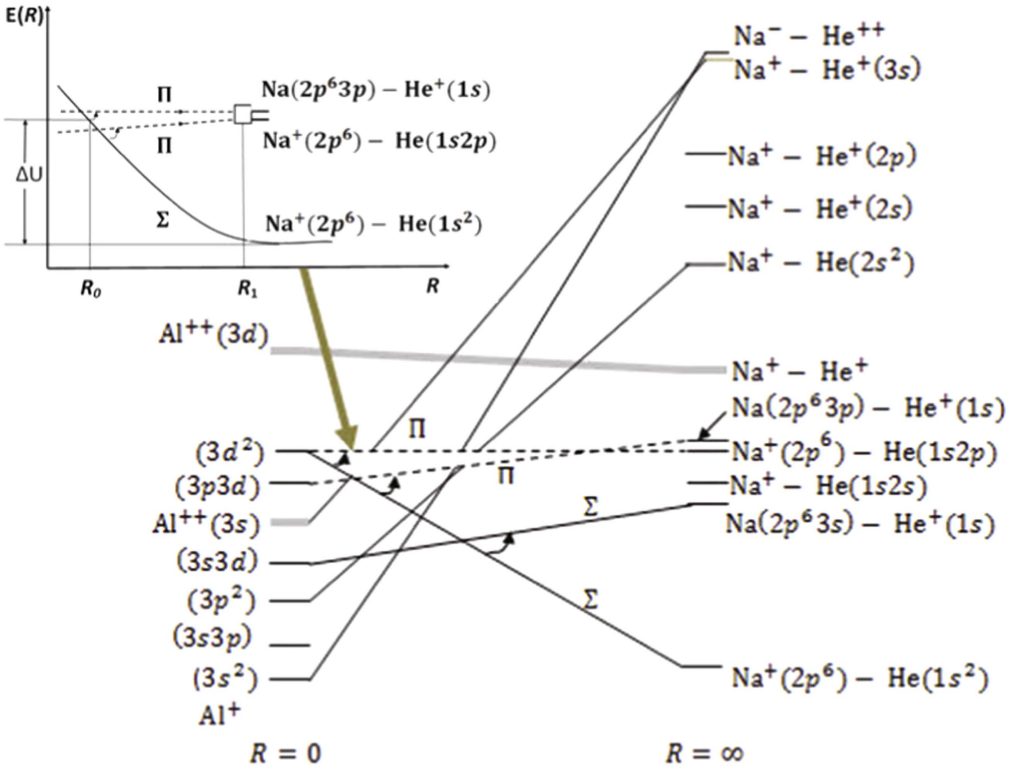

Figure 8. Schematic correlation diagram for some states for the Na^+−He collision system. Solid lines indicate Σ states; dashed lines indicate Π states. The insert at the upper left corner shows the quasi-crossing of the ground state term of the system $Na^+(2p^6) - He(1s^2)$ with the $Na^+(2p^6) - He(1s2p)$ and $Na(2p^6 3p) - He^+(1s)$ terms. The arrow indicates the corresponding terms at the schematic correlation diagram at small internuclear distances.

contributions to the total ionization cross section. To find the contribution of direct ionization $Li^+(1s^2) + Ar(3p^6) \rightarrow Li^+(1s^2) + Ar^+(3p^5) + e$, we use the procedure described in [30]. It should be noted that the expression given in [30] is written in terms of the principal quantum number for a hydrogen-like ion. Therefore, we modify this expression slightly for the estimation of the cross section for the emission of electrons from multi-electron atoms. The final expression which is used below is equation (7) from our previous work [19]. We use this equation for the interpretation of the results for K^+−Ar and for the Na^+−He collision systems in the following subsections as well. Analysis of the correlation diagram of the molecular orbital for the $(LiAr)^+$ system in figure 7 shows that the 3*p* electrons of the Ar atom, whose ionization is considered in the united atom limit, correlate with the 3*d* electrons of the scandium ion Sc^+. The energy E_{nl} of the electrons in the nonadiabatic region was chosen to be equal to that of the 3*d* electrons of the Sc^+ ion. We use data from [33–35] to determine the energy E_{nl} and effective charge Z_{eff} for the 3*d* electrons of the scandium ion Sc^+, being in the states with the electron configuration of a few vacancies. The effective charge Z_{eff} was determined through the interpolation of the data from [35]. For the 3*d* electrons of the scandium ion Sc^+, we obtain $E_{nl} = 35.7$ eV and $Z_{\text{eff}} = 4.8$. With these parameters, using equation (7) from [19], we calculate the cross section for the direct ionization shown in figure 4 that agree with experimental data.

The above procedure was used to estimate the contribution of stripping processes, which are also a source of ejected electrons. The correlation diagram in figure 7 indicates that in the united atom limit the 1*s* state of the Li^+ ion correlates with the 3*d* state of the scandium ion Sc^+. Our calculations for the contribution of the stripping processes with the binding energies from [33, 34] show that at $E = 3.0$ keV, the contribution of the stripping processes to the total ionization cross section is less than 0.4%, while at 6.0 keV it is less than 2%. Therefore, the contribution of the stripping processes are insignificant over the entire energy range studied.

The aforementioned agreement of our calculation for the direct ionization with the experimental data together with the estimation of the portion for the atomic autoionization and the stripping allows us to conclude, that the contribution of direct ionization process to the total cross section for the electron emission is the governing mechanism for the Li^+−Ar collisions.

4.2.2. $K^+ - Ar$ collisions. It follows from the results of the present measurements of the electron ejection cross sections that the liberation of electron with energies in the range of 20–32 eV are strongly related to the ionization in K^+−Ar collisions. The energy-loss spectrum for the K^+−Ar collision (see figure 6) shows the different processes that lead to the ionization of the target atom with aforementioned energies of

electrons. A decisive role may be played by the processes of autoionization and of ionization with the excitation of Ar atoms. These processes are represented by the fourth peak of the energy-loss spectrum. As shown below, the direct ionization and multiple ionization of the target atom does not contribute significantly to the effective cross section for a target atom ionization. To determine the channel and the mechanism of ionization, we estimate the contribution of the direct ionization $K^+(3p^6) + Ar(3p^6) \rightarrow K^+(3p^6) + Ar^+(3p^5) + e$.

An analysis of correlations for molecular orbitals in one-electron approximation for the K^+-Ar system shows that ionization of $3p$ electrons of the Ar atom in the limit of the united atom correlate with the $4d$ electrons of rubidium ion Rb^+. Thus, for the estimation we choose the orbital angular momentum $l = 2$. The binding energy E_{nl} of electrons in the nonadiabaticity region was assumed to be equal to the binding energy of $4d$ electrons of the Rb^+ ion. Since it would be difficult to determine accurately the effective charge Z_{eff} and E_{nl} for the $4d$ electrons of the rubidium ion Rb^+ which are in the excited states with the electron configuration of Ar like ion $[Ar]3d^64p^24f^24d^55f^2$, the effective charge Z_{eff} was determined by the interpolation of the results [31] obtained with the Hartree method [35]. Estimations of the cross section for the direct ionization with these parameters show that at an ion energy of $E = 2$ keV the contribution of the direct ionization to the total ionization cross section is less than 1.5%, while at $E = 7.0$ keV it is less than 2.5%, and hence, its average value does not exceed 3.5×10^{-18} cm^2. This means that this contribution is negligible over the entire energy range studied. According to these calculations and based on our results for the energy of liberated electrons, one can conclude that the primary mechanism for the ionization is related to the decay of autoionization states. As seen from the energy-loss spectrum for the K^+-Ar collision system shown in figure 6, the states with energies of 25–34 eV are excited with a noticeable probability. These energies correspond to the autoionization states of Ar atom with excitation of one $3s$ electron and two $3p$ electrons, with configurations of $3s3p^64s$ and $3p^44s4p$, respectively.

4.2.3. $Na^+ - He$ collisions. The liberation of electrons with energies less than 17 eV is a characteristic of the ionization processes in Na^+-He collisions, as it follows from the measurements of emitted electrons. To reveal the channels and establish the mechanism of the ionization, we estimate the contribution of several inelastic processes that result in emission of slow electrons. Using the Barat–Lichten rules [32] we construct the correlation diagram presented in figure 8. The contribution of the direct ionization $Na^+(2p^6) + He(1s^2) \rightarrow Na^+(2p^6) + He^+(1s) + e$ is estimated following [30]. An analysis of the correlation diagram of molecular orbitals for the Na^+-He system shows that the $1s$ state of the He atom in the limit of the united atom becomes the $2p$ state of the Al^+ ion. Thus, for the estimation of cross section we choose the orbital angular momentum $l = 1$. The binding energy E_{nl} of the electrons in the nonadiabatic region is chosen to be equal to the $2p$ electrons of the aluminum ion Al^+ (28.75 eV). The effective charge Z_{eff} was determined through the interpolation of the results obtained by means of a Hartree calculation [35]. For the $2p$ electrons of the Al^+ ion, we obtain $Z_{\text{eff}} = 3.7$. The estimation of the cross section for the direct ionization with these parameters shows that at an ion energy of 1.5 keV, the contribution of the direct ionization to the total ionization cross section is less than 5.5%, while at 6.5 keV it is less than 7%.

The same procedure is applied to determine the contribution of the electron yield to the measured ionization cross section as a result of stripping of the projectile ions. As can be seen in the diagram in figure 8, the $2p$ state of the Na^+ ion is correlated with the $3d$ state of the Al^+ ion. Consequently, for calculation of the cross section we select $l = 2$, while we take Z_{eff} to be the same as for the $2p$ electrons of the Al^+ ion used in evaluating the ionization cross section. As a result of this calculation, we find that the contribution of stripping to the total electron emission cross section is less than 12% at the energy of 1.5 keV, and does not exceed 17% at the energy of 6.5 keV. Thus, we can conclude that the contribution of the stripping processes, as well as direct ionization processes to the total ionization cross section, is insignificant in the entire energy range interval studied. Other possible sources for liberation of the electrons, like double ionization of the He atom, $Na^+ + He \rightarrow Na^+ + He^{2+} + 2e$, direct two-particle excitation $Na^+ + He \rightarrow Na^{+*}(2p^53s) + He^*(1s2s)$ and capture accompanied by the ionization of the He^+ ion via reaction $Na^+ + He \rightarrow Na + He^{+*} \rightarrow Na + He^{2+} + e$, evidently have a minor effect upon the ionization cross section. There are two reasons for this: 1) the absence of pseudo-crossings of the corresponding quasi-molecular terms with the ground state term, as seen from the diagram in figure 8; 2) the large energy defect for these processes (54 eV, 53.9 eV and 48.9 eV, respectively). Therefore, by systematically evaluating the contribution of various inelastic processes to the ionization of the target atoms in Na^+-He collisions, we find that the ionization may be caused primarily by the decay of autoionization states in an isolated atom. This assessment is supported by the correlation diagram in figure 8 and by the data from [20] as well. According to [20], these states are associated with a direct two electron excitation of the He atom in autoionization state: $Na^+ + He \rightarrow Na^+ + He^{**}(2s^2) \rightarrow Na^+ + He^+ + e$.

4.3. Excitation processes in $K^+ -$ Ar and $Na^+ - He$ collisions

4.3.1. $K^+ - Ar$ collisions. In discussing the mechanism for the Ar $(3p^54s)$ excitation processes in K^+-Ar collisions we use the energy-loss spectrum obtained in our study, and the results reported in [6]. Following [6], we integrated the energy-loss in the range of 11.5–16 eV, and for the sum of Ar excited states $3p^54s$, $3p^54p$ and $3p^53d$ we obtained 7×10^{-17} cm^2. Since the aforementioned excited levels are energetically close as seen in figure 6, it is difficalt to determine of the relative probabilities of their excitation. Moreover, as shown by a qualitative analysis of the energy-loss spectrum (the shape of the peak and the position of its maximum), the levels for the configurations of $3p^54p$ and $3p^53d$ are excited with high probability, while the level for the configuration $3p^54s$ is populated with a

surprisingly small probability, although the level of $3p^5 4s$ state is at a lower energy level than $3p^5 4p$ and $3p^5 3d$, (11.5 − 12 eV and 13–14 eV respectively). This fact, and also the requirement to have reliable data related to the individual channel, which includes the clarification of the contribution of various excitation processes and determination of mechanisms for the processes, motivated us to perform optical measurements for the resonance Ar ($3p^5 4s$) line in the reaction $K^+ + Ar \rightarrow K^+ + Ar^*$.

The analysis of the spectrum for the K^+−Ar collision system in figure 6 shows that the second peak in the energy-loss spectrum with the width of 11.5 − 16 eV corresponds not only to the excitation processes, but also to the direct ionization of the Ar atom (with an ionization potential of 15.7 eV). Our estimation shows that the direct ionization cross section for the K^+−Ar collision system amounts to 2.8×10^{-18} cm^2 . As seen from our results given by curve 1*c* in figure 5, the average excitation cross section for the resonance Ar line in the $3p^5 4s$ state amounts to 1×10^{-17} cm^2. Thus, due to the smallness of the direct ionization cross section as well as the excitation cross section for the resonance Ar($3p^5 4s$) line, compared to the sum of the excitation cross sections 7×10^{-17} cm^2, one can conclude that the dominant role in the Ar excitation is played by the excitation of the $3p^5 4p$ and $3p^5 3d$ states. As for the mechanism for the excitation of the $3p^5 4s$ resonance of the Ar atom, its population is caused by a cascade transition from aforementioned upper laying levels $3p^5 4p$ and $3p^5 3d$ to the 4*s* resonance level.

4.3.2. $Na^+ - He$ collisions. The oscillatory structure of the energy dependence of the cross sections is more pronounced for the Na^+−He collision system. There are results of measurements in figure 5 for two channels: one channel is the capture of the electron in the excited resonant state Na ($2p^6 3p$) in the charge exchange process, while the other one is inelastic channel for a resonant excitation of the target atom He ($1s2p$). The oscillatory behavior of the cross sections arises from a phase-interference effect [2, 28, 29] at the crossing of the charge exchange and excitation of the helium resonance state potential terms, as shown in the insert in figure 8. The difference between the states of the systems $Na^+(2p^6) + He(1s2p)$ and $Na(2p^6 3p) + He^+(1s)$ interacting at large internuclear distance is only 0.3 eV. This means that the observed oscillations are a consequence of the interference of two energetically neighboring vacant excited states of the systems $Na^+(2p^6) + He(1s2p)$ and $Na(2p^6 3p) + He^+(1s)$, which are interacting at large internuclear distance. The results in figure 5 show that the oscillation on the excitation cross sections for the resonance lines of sodium and helium atoms are in antiphase. The curve obtained by adding the excitation cross sections of these lines turns out to be smooth over the entire energy range.

On the other hand, for the realization of a quasi-molecular interference phenomenon, it is necessary that both of these excited terms be populated by the same entrance term. As seen from the correlation diagram in figure 8, this term may correspond to the ground state $Na^+(2p^6) + He(1s^2)$, which, in the limit of united atom, promotes to the autoionization state of aluminum ion $Al^+(3d^2)$. Therefore, the ground state term, which possess Σ symmetry, populates Π terms of the $Na(2p^6 3p) + He^+(1s)$ and $Na^+(2p^6) + He(1s2p)$ states at small internuclear distance due to the rotational Σ − Π transition, and then, at a large *R*, an interaction of the terms with the same Π − Π symmetry takes place.

The experimental results for the excitation cross sections for the resonance lines of sodium and helium atoms, as well as the mechanisms defined for these processes, allow us to obtain additional information regarding the restoration of parameters for the interaction area. For this reason, we use the procedure suggested in [36]. The insert in figure 8 shows the quasi-crossing of the ground state term $Na^+(2p^6) - He(1s^2)$ with the $Na^+(2p^6) - He(1s2p)$ and $Na(2p^6 3p) - He^+(1s)$ terms at small internuclear distances [37]. If one takes into consideration a quasi-crossing of the ground state term and the excitation terms that are populated at small internuclear distance, then the experimental data allows us to determine the mean value of the threshold energy ΔU for the excited states at the average internuclear distance R_0, and the area of the 'rectangular loop' formed by the terms of these states, shown in the insert in figure 8. The area of the 'rectangular loop', which formed the terms of these states, is $\langle \Delta E \cdot R \rangle$, where ΔE is the energy splitting of the terms and *R* is the internuclear distance. The estimation shows that $\Delta U = 70$ eV and $\langle \Delta E \cdot R \rangle \sim 1.4 \times 10^{-7}$ eV cm. The value of ΔU corresponds to the excitation energy at the quasi-crossing of the ground state term and terms of interference states. Using a potential energy curve for the ground state of the system $(NaHe)^+$ from [38] and $\Delta U = 70$ eV determined from our data, one can unambiguously find that the quasi-crossing of the terms occurs at $R \sim 0.5$ Å internuclear distance.

It is well established that, for a small internuclear distance, Σ − Π transitions, related to a rotation of the internuclear axis, are the most important. Under such conditions, the absolute value of the cross section should be small, and by increasing the velocity of the relative motion of the particles it should increase, reaching maxima at comparatively large velocities. Our data confirm this assumption. Moreover, the comparatively large oscillation depth observed in our study, as well as the data reported in [39], support the assumption that at large internuclear distances the interaction of the terms with the same Π − Π symmetry take place, which are populated due to the rotational transition.

5. Summary and conclusions

In this study, we have measured absolute differential and total cross sections for charge-exchange, ionization and excitation processes in Li^+−Ar, K^+−Ar, and Na^+−He collisions, in the energy range of 0.5–10 keV. We have also measured the energy of the electrons liberated in the collisions, and have found that the energy of most of the liberated electrons is below 12 eV for the Li^+−Ar collision, within the interval 20–32 eV for the K^+−Ar collision system, and less than

17 eV for the Na $^{+}$−He collision. The measurements are performed under the same experimental conditions, using a refined version of the condenser plate method, the collision spectroscopy method with angle- and energy-dependent detection of the collision products, and the optical spectroscopy method, with an accurate calibration procedure of the light recording system. The comparison of our measurements with existing experimental and theoretical results were discussed.

The correlation diagrams for the $(LiAr)^{+}$ and $(NaHe)^{+}$ systems were constructed. The experimental data and the schematic correlation diagrams were used to analyze and determine the mechanisms for the charge-exchange, ionization and excitation processes. The contributions of various partial inelastic channels to the total ionization cross section were estimated and a primary mechanism for this process was defined. The contribution of the direct ionization process to the total cross section for the electron emission is the governing mechanism for the Li^{+}−Ar collision. The primary mechanism for the ionization in the K^{+}−Ar collision is related to the decay of the autoionization state. Our results confirm the conclusion of [20], which states that the ionization in the Na^{+}−He collision is related to a direct two electron excitation of the He atom in autoionization state: $Na^{+} + He \rightarrow Na^{+} + He^{**}(2s^2) \rightarrow Na^{+} + He^{+} + e$.

The energy-loss spectrum was applied to estimate the relative contribution of different inelastic channels and to determine the mechanisms for the ionization and for some excitation processes. The main mechanism for the excitation of the $3p^5 4s$ resonance state of the Ar atom in the K^{+}−Ar collision is related to the cascade transition from upper laying levels $3p^5 4p$ and $3p^5 3d$ to the $4s$ resonance level. The oscillatory structure of the energy dependence of the cross sections is most pronounced for the Na^{+}−He collision system. This behavior is observed in the excitation cross section for the helium resonance line ($\lambda = 58.4$ nm, $2p - 1s$ transition), for the transition $Na^{+} + He \rightarrow Na^{+}(2p^6) + He(1s2p)$, and for the sodium doublet lines ($\lambda = 589.0$ nm and $\lambda = 589.6$ nm, $3p - 3s$ transition) for the transition in Na^{+}−He charge exchange reaction. We conclude that this phenomenon is a consequence of interference of two very energetically close states: namely, the excited states of the $Na^{+}(2p^6) + He(1s^2) \rightarrow Na(3p) + He^{+}(1s)$ and $Na^{+}(2p^6) + He(1s^2) \rightarrow Na^{+}(3p^6) + He(1s2p)$ systems, which are separated only by 0.3 eV.

The results of our experimental studies show that the charge-exchange processes occur with high probabilities, and electrons are predominately captured in the ground state of the resultant atom in the region of pseudocrossing of potential curves of Σ symmetry. The results for the charge-exchange and ionization processes show that in the entire energy range, the cross section for the quasisymmetric K^{+}−Ar collision system is greater than for the largely asymmetric Li^{+}−Ar and Na^{+}−He collision systems. Moreover, based on our experimental data for the considered collision systems, it is clear that the cross sections for charge-exchange processes are always larger for a symmetric collision system than for a largely asymmetric one. The results for excitation functions lead to the conclusion that the cross section in the case of the quasisymmetric K^{+}−Ar collision system is greater than the cross section for the largely asymmetric Na^{+}−He collision system.

Acknowledgments

We would like to thank A Weiss for help with editing the manuscript. This work was supported by the Georgian National Science Foundation under the Grant No. 31/29 (Reference No. Fr/219/6-195/12). RYaK and RAL gratefully acknowledge support from the International Research Travel Award Program of the American Physical Society, USA.

ORCID iDs

Roman Ya Kezerashvili https://orcid.org/0000-0002-0011-4062

References

[1] Ogurtsov G N and Kikiani B I 1966 *Tech. Phys.* **11** 362
[2] Bobashev S V 1970 *Sov. Phys. JETP Lett.* **11** 260
Bobashev S V 1970 *Phys. Lett.* A **31** 204
[3] Bobashev S V and Kritiskii V A 1970 *JETP Lett.* **12** 189
[4] Matveev V B and Bobashev S V 1970 *Sov. Phys. JETP* **30** 829
[5] Francois R, Dhuicq D and Barat M 1972 *J. Phys. B: At. Mol. Phys.* **5** 963
[6] Afrosimov V V, Bobashev S V, Gordeev Y S and Lavrov V M 1972 *Sov. Phys. JETP* **35** 34
[7] Kita S, Noda K and Inouye H 1975 *J. Chem. Phys.* **63** 4930
[8] Afrosimov V V, Gordeev Yu S and Lavrov V M 1976 *Sov. Phys. JETP* **41** 860
[9] Odom R, Caddick J and Weiner J 1977 *Phys. Rev.* A **15** 1414
[10] Sidis V, Stolterfoht N and Barat M M 1977 *J. Phys. B: At. Mol. Phys.* **10** 2815
[11] Jorgensen K, Andersen N and Olsen J 1978 *J. Phys. B: At. Mol. Phys.* **11** 3951
[12] Olsen J O *et al* 1979 *Phys. Rev.* A **19** 1457
[13] Kikiani B I *et al* 1985 *Tech. Phys.* **30** 934
[14] Kita S and Shimakura N 1997 *Phys. Rev.* A **55** 3405
[15] Kita S, Gotoh S, Shimakura N and Koseki S 2000 *Phys. Rev.* A **62** 032704
[16] Lomsadze R A, Gochitashvili M R, Kvizhinadze R V, Mosulishvili N O and Bobashev S V 2007 *Tech. Phys.* **52** 1506
[17] Kita S *et al* 2007 *J. Phys. Soc. Japan.* **76** 044301
[18] Kita S, Hatada T, Shiraishi Y and Shimakura N 2013 *J. Phys. Soc. Japan.* **82** 124301
[19] Lomsadze R A, Gochitashvili M R, Kezerashvili R Ya, Mosulishvili N O and Phaneuf R 2013 *Phys. Rev.* A **87** 042710
[20] Kita S, Hattori T and Shimakura N 2015 *J. Phys. Soc. Japan* **84** 014301
[21] Lomsadze R A, Gochitashvili M R and Kezerashvili R Ya 2015 *Phys. Rev.* A **92** 062703
[22] Gochitashvili M, Lomsadze R, Lomsadze B, Mosulishvili N, Sakhelashvili G *et al* 2004 *Georgian Electron. Sci. J.: Phys.* **2** 162
[23] Gochitashvili M R, Jaliashvili N, Kvizhinadze R V and Kikiani B I 1995 *J. Phys. B: At. Mol. Phys.* **28** 2453

[24] Ajello J M and Franklin B 1985 *J. Chem. Phys.* **82** 2519
[25] Avakyan S V, Il'in R N, Lavrov V M and Ogurtsov G N 1999 *Collision Processes and Excitation of UV Emission from Planetary Atmospheric Gases: A Handbook of Cross Section* (Amsterdam: Gordon and Breach Science) p 344
[26] Gochitashvili M R, Kezerashvili R Ya and Lomsadze R A 2010 *Phys. Rev.* A **82** 022702
[27] Kita S, Izawa M and Inouye H 1983 *J. Phys. B: At. Mol. Phys.* **16** L499
[28] Rosenthal H and Foley H M 1969 *Phys. Rev. Lett.* **23** 1480
[29] Ankudinov V A, Bobashev S V and Perel' V I 1971 *Zh. Eksp. Teor. Fiz.* **60** 906
Ankudinov V A, Bobashev S V and Perel' V I 1971 *Sov. Phys JETP* **33** 490
[30] Solov'ev E A 1981 *Sov. Phys., JETP* **54** 893
[31] Barat M, Dhuieq D, Francois R and Sidis V 1973 *J. Phys. B: At. Mol. Phys.* **6** 2072
[32] Barat M and Lichten W 1972 *Phys. Rev.* A **6** 211
[33] Schippers S *et al* 2003 *Phys. Rev.* A **67** 032702
[34] Müller A 2008 *Adv. At. Mol. Opt. Phys.* **55** 293
[35] Hartree D R 1957 *The Calculation of Atomic Structures* (New York: Wiley)
[36] Tolk N H, White C W, Neff S H and Lichten N 1973 *Phys. Rev. Lett.* **31** 671
[37] Bobashev S V 1979 *Adv. At. Mol. Opt. Phys.* **14** 341
[38] Nikulin V K and Tsarev Y N 1975 *Chem. Phys.* **10** 433
[39] Bobashev S V and Kharchenko V A 1976 *Sov. Phys. JETP* **44** 693